

# Re-M3Dr: Rebalanced MultiModal Mean Deviation Regression

Haojie Yin<sup>1</sup>, Chengcheng Feng<sup>1</sup>, Tianyi Liu<sup>2</sup>, and Tianqi Zhang<sup>3</sup> Kaizhu Huang<sup>1</sup>

<sup>1</sup> Duke Kunshan University, China

<sup>2</sup> Xi'an Jiaotong-Liverpool University, China

<sup>3</sup> Soochow University

**Abstract.** Mean Deviation (MD) is a critical metric for assessing visual field loss in ophthalmology. While previous work has focused solely on predicting MD from Optical Coherence Tomography (OCT), it is intuitive to assume that combining OCT with another imaging of fundus photography (FP) could improve performance, as two ophthalmic medical imaging provide complementary information. This is particularly expected when sophisticated multi-objective optimization is applied, as documented in common multimodal classification. Surprisingly, our investigations reveal that multimodal fusion in this medical imaging scenario performs worse than unimodal model. Through detailed analysis, we identify the root cause as a coupled imbalance between data distribution and modality learning conflict. This imbalance distorts the optimization landscape, leading to unstable training. To address this challenge, we propose the method of Rebalanced MultiModal Mean Deviation Regression (Re-M3Dr), a novel multimodal regression framework. We enhance unimodal representation through adaptive margin based supervised contrastive learning. Then, our framework stabilizes the joint optimization with the sharpness-aware gradient modulation. Experimental results on both public and private clinical datasets show average 29% reduction in MSE compared to SOTA multimodal learning methods, demonstrating the superiority of Re-M3Dr. The code is available in the supplementary materials.

**Keywords:** Data imbalance · Multimodal learning · Regression

## 1 Introduction

Mean Deviation (MD) value is a widely used clinical indicator for quantifying visual field loss in ophthalmology [1]. While prior research [15] has primarily focused on unimodal MD prediction using Optical Coherence Tomography (OCT) images, it seems reasonable to hypothesize that integrating multiple modalities could enhance performance. To this end, we investigate multimodal MD prediction by combining fundus photography (FP) and OCT. Interestingly, our empirical observations indicate that multimodal models underperform compared

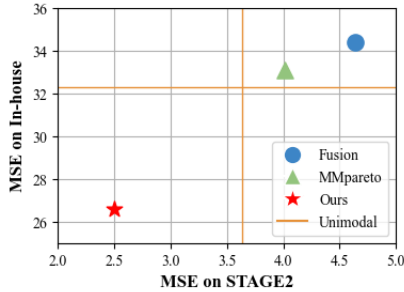


Fig. 1: Mean Squared Error on MD regression datasets.

to their single-modality counterparts (see Fig. 1). This phenomenon, called *multimodal learning imbalance*, is actually well-documented in the multimodal learning literature [14], often attributed to a learning imbalance between modalities. In such cases, one modality tends to dominate the optimization process, while others are underutilized or even introduce hindrances to learning, resulting in ineffective multimodal fusion and degraded model performance [10].

To address multimodal learning imbalance, multi-objective optimization (MOO) has emerged as a promising solution. By integrating both unimodal and multimodal gradients through Pareto optimization, MOO enables the model to balance the conflicting objectives of each modality. A representative method, MMPareto [13], further improves this framework by modulating the magnitude of the integrated gradients, thereby enhancing generalization and overall performance. Naturally, we applied MMPareto to our MD prediction task. However, unexpectedly, MMPareto still significantly underperforms the best unimodal baseline, as demonstrated in Fig. 1.

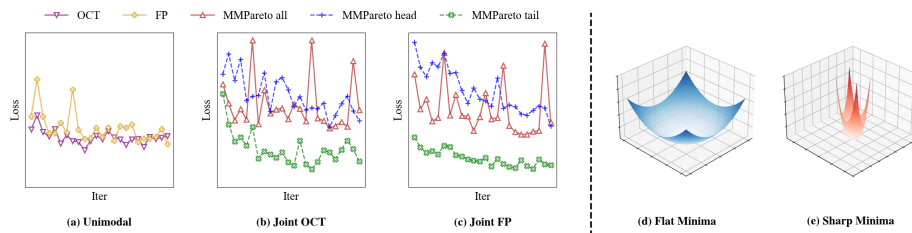


Fig. 2: (a) Loss changes during unimodal training; (b) and (c) Loss changes corresponding to the unimodal head under the MMPareto multimodal joint learning. The figure shows three sets: red represents the loss changes when training with all data, blue represents training with only head-class data, and green represents with only tail-class data. It can be observed that the outputs of unimodal prediction heads with all data are highly unstable.

To investigate this intriguing failure, we conducted a series of analytical experiments. During training, we observed that the unimodal prediction heads within the MMPareto framework displayed highly unstable and oscillatory outputs, as shown in Fig. 2(b)-(c). These fluctuations indicate that the optimization process frequently converges to sharp minima (see Fig. 2(e)), which significantly undermines the network’s generalization ability [5, 18]. Further inspection of the dataset reveals a long-tailed distribution, where samples are heavily concentrated in certain MD regions while other regions remain sparsely represented. To delve deeper into this issue, we trained the multimodal network separately on head-class and tail-class data. In both cases, the oscillations in the unimodal outputs were markedly reduced. Furthermore, when training unimodal networks on the complete long-tailed dataset, their predictions remained stable in Fig. 2(a). These findings indicate that the instability is not caused by issues with data quality or individual modalities. Instead, it stems from the **interplay between data imbalance and learning imbalance**. Namely, data imbalance critically destabilizes multimodal training, increasing susceptibility to sharp minima. Simultaneously, the learning imbalance leads to poor generalization on imbalance data. This mutual amplification between the two forms of imbalance significantly degrades model performance.

To better understand this phenomenon, we analyze the optimization dynamics induced by this coupled imbalance. The long-tailed data distribution introduces large variance in unimodal gradients, while learning imbalance across modalities further increases the discrepancy among these gradients. When such inconsistent gradients are aggregated through multi-objective optimization, the resulting optimization direction exhibits highly anisotropic gradient statistics, which in turn distort the effective loss landscape and produce numerous sharp minima, a phenomenon also observed in long-tailed learning and multi-objective optimization settings [11, 17].

This observation reveals a fundamental limitation of existing gradient modulation methods such as MMPareto. These approaches implicitly assume that sharp minima are surrounded by relatively flat neighborhoods, so that injecting noise into gradients can help the optimizer escape sharp basins. However, under the distorted loss landscapes induced by coupled imbalance, this assumption no longer holds. Even regions that are relatively flat may appear sharp in certain directions, and the joint loss surface becomes populated with many sharp minima. Consequently, instead of escaping sharp regions, gradient modulation may cause the optimization trajectory to oscillate among them, resulting in unstable training and degraded generalization.

Motivated by these findings, we propose **Rebalanced MultiModal Mean Deviation Regression (Re-M3Dr)**, a two-stage framework designed to stabilize multimodal learning under coupled imbalance. The key idea of Re-M3Dr is to decouple unimodal representation stabilization from multimodal optimization. Specifically, the first stage focuses on strengthening unimodal representations under long-tailed data, while the second stage performs stable multimodal fusion guided by sharpness-aware gradient modulation. This design mitigates the

mutual amplification between data imbalance and learning imbalance, thereby improving both optimization stability and generalization performance.

In the first stage, we enhance unimodal representation learning through **Adaptive-Margin (AM)** Supervised Contrastive Learning. Existing methods often overlook the role of sample boundaries in representation learning; once the model has acquired sufficient discriminative ability, capturing finer distinctions requires pushing apart nearby samples rather than continuing to pull them closer as in the early stages. To address this issue, AM introduces adaptive margins tailored to the long-tailed distribution, enabling the model to better separate boundary samples. This mechanism improves representation quality for minority samples and stabilizes unimodal gradient signals, providing a reliable foundation for subsequent multimodal learning.

In the second stage, we perform multimodal fusion using multi-objective optimization enhanced with **Sharpness-aware Gradient Modulation (SGM)**. Unlike existing gradient modulation methods such as MMPareto, SGM dynamically adjusts the modulation strength according to the sharpness of the loss surface. This enables the optimizer to escape sharp minima while maintaining stable convergence in relatively flat regions, effectively addressing the distorted loss landscapes induced by coupled imbalance.

To the best of our knowledge, we are the **first** to investigate the data imbalance problem in multimodal OCT and FP MD prediction, revealing a critical coupled imbalance through both theoretical analysis and empirical observations, which explains why existing multimodal optimization methods may fail. To validate our analysis and the effectiveness of the proposed method, we conduct extensive experiments on **three** regression datasets with coupled imbalance. Furthermore, we evaluate our approach on **eight** datasets across four additional settings, including natural image benchmarks and other medical modalities, demonstrating strong generalization and robustness. The results further confirm that the two modules effectively tackle the decoupled subproblems of data imbalance and learning imbalance, enabling stable and balanced multimodal learning.

## 2 Related Work

### 2.1 Contrastive Learning for Imbalance Data

Contrastive learning has shown notable success in long-tailed regression tasks [8, 12]. For example, EchoMEN [7] incorporates label distance to define positive pairs, and then determines the degree of separation between samples based on their distance. However, these methods overlook the impact of sample boundaries on representation learning. In the later stages of training, model has gained sufficient discriminative ability. At this point, to help the model capture finer distinctions, it becomes necessary to push apart nearby samples rather than pull them closer as in the early stages.

## 2.2 Multimodal Learning Imbalance

The simplest way to address learning imbalance is to control the fitting speed of different modalities, giving the harder modality sufficient time to converge. OGM-GE introduces separate output heads for each modality to monitor their individual learning states and down-weight the dominant unimodal gradient, thereby synchronizing learning speeds [10]. MMPareto further improves this by adopting Pareto optimality from multi-task learning, encouraging each unimodal gradient to align toward a Pareto front [13]. This promotes better utilization of all modalities and mitigates optimization conflict.

## 3 Theoretical Analysis

### 3.1 Preliminary

We consider a MOO-based multimodal optimization problem with a set of unimodal losses  $\{L_u^{(k)}(\theta)\}_{k=1}^K$  and a multimodal loss  $L_m(\theta)$ . The joint objective is defined as

$$L(\theta) = L_m(\theta) + \sum_{k=1}^K \alpha_k L_u^{(k)}(\theta), \quad (1)$$

where  $\alpha_k$  controls the proportion of the unimodal loss set relative to the multimodal loss.

### 3.2 Optimization Failure Analysis

We first borrow Proposition 1 from [13]:

**Proposition 1 (Necessity of Gradient Amplification in Pareto Optimization).** *MOO-based formulate joint training as the following problem:*

$$\min_{\theta} \mathbf{f}(\theta) = \gamma \left( L_m(\theta), \alpha_1 L_u^{(1)}(\theta), \dots, \alpha_k L_u^{(k)}(\theta) \right)^\top.$$

*Let  $g_t$  denote the Pareto descent direction that balances all objectives. In MOO-based multimodal learning, training requires stronger gradient amplification factor  $\gamma$  to promote escaping sharp minima.*

However, in long-tailed settings, the joint loss landscape constructed via MOO becomes highly rugged and anisotropic. Although gradient modulation can help the optimizer escape sharp minima, under such distorted geometry it overreact and overshoot the flatter regions, ultimately destabilizing unimodal optimization and hindering convergence.

**Proposition 2 (Failure of Blind Gradient Modulation ).** *Assume  $F$  is  $L$ -smooth around  $\theta_t$ . Let  $\delta > 0$  denote the minimal step magnitude required to escape the basin of a sharp minimum. When the loss landscape contains sharp*

directions, there does not exist a fixed modulation factor  $\gamma > 0$  satisfying both simultaneously guarantee optimization stability and the ability to escape sharp minima. Therefore, MOO-based methods fail in Long-tailed multimodal regression setting.

*Proof.* The proof can be seen in Appendix.  $\square$

*Remarks.* The above propositions reveal a clear trade-off. To balance multimodal learning, we adopt MOO and increase  $\gamma$ , which helps multimodal branches escape sharp regions. However, this simultaneously reduces the unimodal branch’s ability to settle into flatter minima, leading to instability in long-tailed data distribution. Ultimately, this undermines joint training and explains the counterintuitive result that MOO-based methods perform worse than unimodal baselines in coupled imbalanced multimodal regression scenarios.

## 4 Method

We consider a multimodal regression task with a training dataset consisting of  $N$  instances. Each instance  $x_i = \{x_i^{(k)}\}_{k=1}^K$ , where  $x_i^{(k)}$  represents the  $k$ -th modality and  $K$  denotes the number of modalities, with a continuous target value  $y_i \in \mathbb{R}$ .

To address the coupled imbalance problem in multimodal learning, we propose Re-M3Dr, a two-stage framework that decouples unimodal representation stabilization from multimodal optimization. Specifically, the first stage focuses on strengthening unimodal representations through contrastive pretraining to mitigate the impact of data imbalance and enhance representation quality. The second stage performs multimodal fusion using SGM, enabling stable and balanced joint learning under the distorted loss landscapes induced by coupled imbalance. Re-M3Dr is equipped with theoretical convergence guarantee, which aligns well with our empirical findings. The guarantee explains why Re-M3Dr converges more stably in relatively flat regions, while still preserving a strong capability to escape sharp minima under coupled imbalance regression. The detailed proof is provided in Appendix.

### 4.1 Adaptive Margin Supervised Contrastive Pretraining for Data Imbalance Regression

We adopt supervised contrastive learning to pretrain unimodal encoders. Regression lacks clear label boundaries to distinguish positive and negative samples. So it is necessary to distinguish them based on the label distance. If the margin is too large, the model may incorrectly align features of dissimilar samples, hindering convergence. Conversely, an overly small margin leave the model with insufficient similar samples to effectively capture representative features, especially for tail-class. Therefore, we introduce adaptive margin to define positives and negatives dynamically based on the label distance and training time as

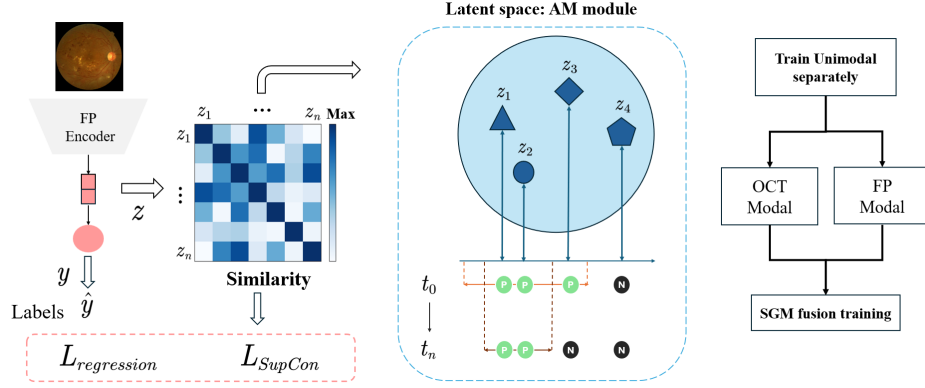


**Fig. 3:** Illustration of adaptive margin in supervised contrastive learning. P: positive; N: negative. Early in training,  $z_1$  and  $z_3$  are positives for  $z_2$ , while  $z_4$  is negative. As training progresses, the margin shrinks, and distant positive  $z_3$  becomes negative.

shown in Fig. 3. For a training batch with indices  $i \in I$ , we define the positive and negative set for sample  $i$  as:

$$P(i) := \{j \in I \mid |y_i - y_j| < m(t)\}$$

$$N(i) := \{j \in I \mid |y_i - y_j| \geq m(t)\}$$

where  $m(t)$  is a time-dependent margin that defines the similarity threshold between labels. It remains fixed in the early training stage and decays exponentially afterward:

$$m(t) = \begin{cases} m_0 & \text{if } t < t_n \\ m_0 \cdot \exp(-\beta \cdot (t - t_n)) & \text{if } t \geq t_n \end{cases}$$

Here,  $m_0$  is the initial margin,  $\beta$  is the decay rate, and  $t_n$  is the warm-up duration before margin decay begins. The feature representation is used to construct the similarity matrix.  $L_{\text{regression}}$  serves as the supervised signal.  $z_p$  represents the feature vector of positive sample, and  $z_a$  denotes all anchor features in the batch used for normalization. Then, we apply the standard supervised contrastive loss:

$$\mathcal{L}_{\text{SupCon}} = -\log \frac{\exp(z_i \cdot z_p / \tau)}{\sum \exp(z_i \cdot z_a / \tau)}$$

where  $z_i$  is the projected feature representation for sample  $x_i$ ,  $\tau$  is the temperature parameter. We further introduce regression loss  $L_{\text{regression}}$  to compose supervised sign. The total loss for Stage 1 is:

$$\mathcal{L} = \mathcal{L}_{\text{regression}} + \lambda \cdot \mathcal{L}_{\text{SupCon}}$$

This two-term loss enables the encoder to learn smooth and discriminative features, which serve as a solid foundation for multimodal fusion in the next stage.

## 4.2 Robust Gradation Modulation for Multimodal Learning

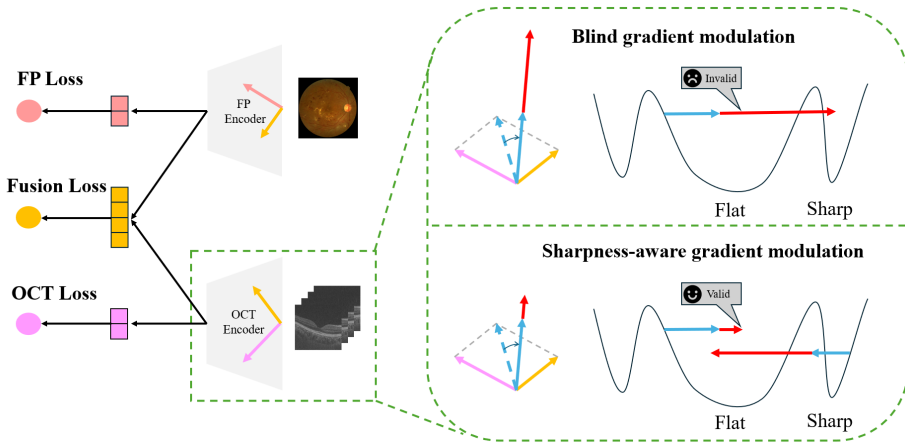


**Fig. 4:** Illustration of SGM. For example, given the multimodal and OCT loss, the network computes the Pareto-optimal direction via MOO. Mmpareto amplifies the combined gradient to compensate for the lower noise in the joint training. But this blind amplification may prevent convergence to flat minima. SGM adjusts the modulation scale based on loss geometry, enabling both escape from sharp minima and stable convergence to flat regions.

**Sharpness-aware Gradient Modulation (SGM).** As illustrated in Fig. 4, our approach dynamically adjusts the magnitude of integrated gradients according to the sharpness of the local loss surface. Given a minibatch  $\mathcal{B}$ , the network produces one multimodal prediction and  $K$  unimodal predictions, yielding a multimodal regression loss and a set of unimodal losses. SGM adaptively adjusts the gradient modulation strength according to the local sharpness of the loss surface. Starting from the current parameter  $\theta_t$ , we probe a nearby peak and valley by performing a few steps of *normalized* gradient ascent and descent on  $L(\theta)$ , respectively. Let  $\mathcal{T}^+$  and  $\mathcal{T}^-$  denote the two one-step perturbed points obtained by normalized gradient ascent and descent from  $\theta_t$ , respectively. We compute a normalized perturbation

$$\Delta_t = \epsilon \cdot \frac{\nabla_{\theta} L(\theta_t)}{\|\nabla_{\theta} L(\theta_t)\| + \varepsilon},$$

and evaluate the loss at the two perturbed parameters  $\theta_t^+ = \theta_t + \Delta_t$  and  $\theta_t^- = \theta_t - \Delta_t$ . We then define the sharpness score as  $s_t = L(\theta_t^+) - L(\theta_t^-)$ .

To make the modulation robust over time, we maintain a sliding window  $\mathcal{W}$  of recent sharpness scores and compute a normalized rescaling factor

$$\gamma_t = \text{clip}\left(\gamma_{\text{base}} \cdot \frac{s_t}{\text{median}(\mathcal{W})}, \gamma_{\text{min}}, \gamma_{\text{max}}\right),$$

where  $\gamma_{\text{base}}$  controls the overall scale and  $[\gamma_{\text{min}}, \gamma_{\text{max}}]$  prevents extreme rescaling. Intuitively,  $\gamma_t$  increases when the current region is sharper than the recent history, and decreases in relatively flat regions, enabling the optimizer to escape sharp minima while avoiding over-modulation in flat basins. To handle conflicts between unimodal and multimodal objectives, SGM explicitly separates and reweights their gradients on the shared parameters. For each objective  $\ell \in L_m \cup \{L_u^{(k)}\}_{k=1}^K$ , we backpropagate  $\ell$  independently and record the gradient on shared parameters, resetting gradients after each backward pass. This yields a multimodal gradient  $g^{\text{mm}}$  and a set of unimodal gradients  $\{g^{(k)}\}_{k=1}^K$ . We aggregate unimodal gradients as  $g^{\text{uni}} = \sum_{k=1}^K g^{(k)}$ . We then compute the cosine similarity between  $g^{\text{mm}}$  and  $g^{\text{uni}}$  to detect objective conflicts:

$$\cos \beta = \frac{\langle g^{\text{mm}}, g^{\text{uni}} \rangle}{\|g^{\text{mm}}\| \|g^{\text{uni}}\|}.$$

If  $\cos \beta < 0$ , the two objectives disagree and we solve a standard MinNorm problem to obtain Pareto-optimal weights  $(\alpha_{\text{mm}}, \alpha_{\text{uni}})$  that minimize the norm of the combined gradient while respecting both objectives. Otherwise, when the gradients are roughly aligned, we set uniform weights  $(\alpha_{\text{mm}}, \alpha_{\text{uni}}) = (0.5, 0.5)$  to avoid unnecessary overhead. The Pareto-integrated gradient for each shared parameter  $\theta_i$  is then  $g_i = 2\alpha_{\text{mm}} g_i^{\text{mm}} + 2\alpha_{\text{uni}} g_i^{\text{uni}}$ , where the factor 2 ensures that when  $\alpha_{\text{mm}} = \alpha_{\text{uni}} = 0.5$ , we recover the usual sum of the multimodal and unimodal gradients. To keep the update scale consistent with the baseline optimizer dynamics, we compute the baseline gradient by backpropagating the total loss in Eq. (1):  $g^{\text{base}} = \nabla_{\theta} L(\theta_t)$ . For each shared parameter  $\theta_i$ , SGM normalizes the Pareto-integrated direction to match the baseline magnitude and then applies the sharpness-aware factor:

$$\nabla_{\theta_i} \leftarrow \gamma_t \cdot \frac{\|g_i^{\text{base}}\|}{\|g_i\| + \epsilon} \cdot g_i,$$

where  $\epsilon$  is a small constant for numerical stability. This step preserves the direction determined by Pareto integration while controlling the effective step size using both the baseline gradient scale and the local sharpness. Finally, the optimizer updates  $\theta$  with the rescaled gradients for the next iteration.

## 5 Experiment

To validate our analysis and the effectiveness of Re-M3Dr, we conduct experiments under five distinct settings. For validate Re-M3Dr system, (1) Coupled

imbalance regression. We study coupled imbalance on the only public multimodal MD dataset and our in-house clinical MD dataset. In addition, we observe the same coupled-imbalance phenomenon on the CHIMERA Challenge dataset. While prior works have reported cases where multimodal learning underperforms using fewer modalities, they just attribute the gap to extra modality noise. For other setting results, we report them in Appendix. (2) Standard multimodal regression benchmarks. We further evaluate on CT Slices and Superconductivity, two widely-used multimodal regression benchmarks. We also report CMU-MOSI, a natural-modality sentiment analysis multimodal regression dataset. Our sub-modules have strong generalization ability. For Validate AM (3) Unimodal long-tailed regression. We conduct experiments on bone age assessment in RSNA 2017 and age regression in AgeDB dataset. For validate SGM, we test on (4) multimodal classification, including the medical glaucoma grading dataset GAMMA and the learning imbalanced natural-modality dataset CREMA-D. (5) Multi-task learning. Finally, we evaluate on MultiMNIST to examine robustness under task interference.

### 5.1 MD Regression Datasets

We adopt the multimodal MD public dataset from MICCAI 2024 STAGE2 Challenge. Each sample contains a set of OCT slices and FP, along with structured tabular information including age, gender, laterality (left or right eye), glaucoma stage, and the MD value. In addition, we evaluate our method on a private in-house dataset collected from a local hospital. We use 500 samples for training and 200 samples for testing.

### 5.2 Setting

We took three classic regression metrics:  $R^2$ , MSE, MAE. During training, we use a combination of SMAPE and  $R^2$  as loss function. All experiments are conducted on a NVIDIA L20 GPU. We exploit ResNet34 as the backbone network, following the [13]. The results of integrating different backbone networks (e.g., ViT) are provided in the Appendix. The batch size is set to 8. We adopt the Adam optimizer and we also report the performance under different optimizers in the Appendix. Additional details about the datasets, baseline description and code can be found in the supplementary material.

### 5.3 Comparison with SOTA Methods

**Comparison Baselines.** To comprehensively evaluate the effectiveness of our proposed method, we compare it against a diverse set of baselines from multiple perspectives: 1). Multimodal Optimization Methods: OGM-GE and MM-Pareto address learning imbalance through multi-objective optimization. 2). Ophthalmology-Specific Methods: Eyemost [20] and EyemostPlus [19] fuse OCT

**Table 1:** Performance comparison on multimodal MD datasets. Best results are in **bold**, second best of baseline are underlined.

Method	Modal		STAGE2 Dataset			In-house Dataset		
	OCT	FP	$R^2 \uparrow$	MSE $\downarrow$	MAE $\downarrow$	$R^2 \uparrow$	MSE $\downarrow$	MAE $\downarrow$
Baseline	✓		0.420	5.01	1.59	-0.303	33.4	5.15
		✓	<u>0.605</u>	3.63	1.38	-0.146	32.6	5.25
	✓	✓	0.371	4.64	1.52	-0.283	34.2	5.30
OGM-GE [10]	✓	✓	0.468	3.78	1.43	-0.122	31.2	5.42
MMPareto [13]	✓	✓	0.532	4.01	1.39	-0.046	33.3	5.00
EyeMoSt [20]	✓	✓	0.478	5.47	1.45	0.033	29.7	5.17
EyeMoSt+ [19]	✓	✓	0.381	3.97	1.44	-0.015	32.4	5.40
SAM [3]	✓	✓	0.537	3.74	1.32	-0.081	32.8	5.15
ImbSAM [16]	✓	✓	0.276	4.14	1.56	-0.032	32.1	5.43
SSE-SAM [9]	✓	✓	0.532	3.46	1.38	-0.146	30.0	5.58
EGVFI [15]	✓		0.390	3.78	1.53	-0.168	32.1	5.40
SF3D [6]	✓		0.168	3.75	1.53	-0.030	31.4	5.26
SimCLR [2]	✓	✓	0.215	4.47	1.58	-0.148	33.4	5.65
ConR [4]	✓		0.358	5.20	1.60	0.036	33.4	5.10
		✓	0.504	3.48	1.40	-0.055	30.3	5.23
	✓	✓	0.483	3.90	1.48	-0.085	37.3	5.33
EchoMEN [7]	✓		0.053	5.02	1.66	0.062	29.2	5.03
		✓	0.569	<u>3.18</u>	<u>1.30</u>	<u>0.109</u>	<u>27.3</u>	<u>5.04</u>
	✓	✓	0.455	4.21	1.51	0.055	28.9	5.39
<b>Re-M3Dr</b>	✓		0.340	4.79	1.54	0.030	30.2	5.56
		✓	0.601	2.87	1.23	0.075	27.0	4.77
	✓	✓	<b>0.626</b>	<b>2.50</b>	<b>1.16</b>	<b>0.229</b>	<b>26.5</b>	<b>4.62</b>

and fundus images via evidential learning for classification tasks. 3). Sharpness-Aware Optimization: SAM [3] estimates sharpness via perturbation-based approximation, while ImbSAM [16] and SSE-SAM [9] adapt SAM to long-tailed settings. 4). Mean Deviation Prediction Models: EGVFI [15] and SF3D [6] are 3D-based models designed for MD value prediction. 5). Contrastive Learning Methods: SimCLR [2] adopts an unsupervised pretraining strategy. EchoMen [7] is a regression method specifically designed for long-tailed medical data. ConR [4] transfers label relationships into the feature space. The latter two methods are based on supervised contrastive learning.

**Analysis.** Across both public and private datasets, multimodal baselines underperform compared to their unimodal counterparts. Notably, OGM-GE achieves slightly better results than MMPareto, despite its simpler design. This aligns with our analysis: in the presence of an extremely distorted loss landscape, overly aggressive optimization strategies tend to converge to sharp minima and suffer

from poor generalization. In contrast, the more conservative nature of OGM-GE helps it navigate such extreme landscapes more reliably.

We further observe that contrastive learning provides substantial improvements in the unimodal setting. However, its performance degrades and fails to surpass the unimodal results in joint optimization. This validates our claim that addressing only one form of imbalance is insufficient—without explicitly tackling the other one, performance gains remain limited.

As expected, 3D-based models outperform all other OCT-only methods due to their ability to capture richer spatial context. In contrast, the other methods utilize 2D networks, which inherently limit the representational power for volumetric OCT data.

We also notice that all methods exhibit degraded performance on the private dataset. This can be attributed to two primary factors: (1) the private dataset exhibits a wider range of MD value distribution, and (2) the data distribution is severely distorted., which poses a greater challenge for model generalization. Despite in real-world clinical scenarios, our method consistently achieves SOTA performance. Our approach reduces the average MSE by 29% compared to MM-Pareto, which demonstrates its strong capability. Further evaluations, including cost–time efficiency and detailed long-tailed performance analysis, are presented in the Appendix.

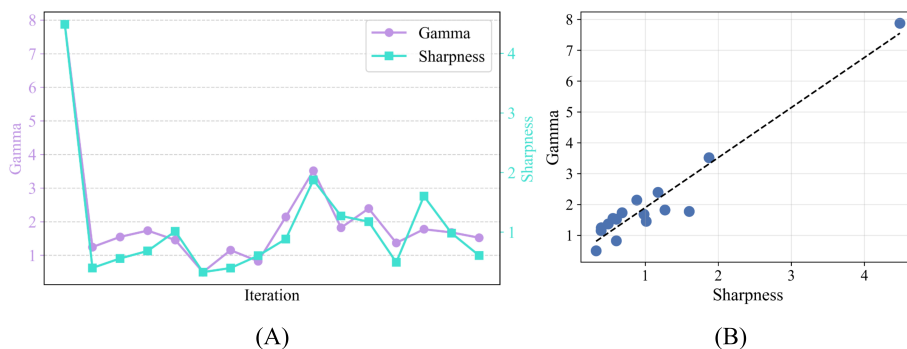
#### 5.4 Ablation

We conduct ablation study on the STAGE2 dataset to investigate the contribution of each component in table 2. The variations include: (a) w/o SGM: During contrastive pretraining, we replace the AM with a fixed margin throughout training, while keeping SGM jointly learning. (b) w/o SGM (Unimodal Only): We remove the SGM module and just use contrastive pretraining for unimodal learning. (c) w/o SGM (Fusion): After contrastive pretraining, we apply a naive joint optimization without SGM during multimodal training. (d) AM w/ MP : We retain the AM in the first stage but replace our SGM module in the second stage with the MMPareto method (MP). Each ablation leads to performance degradation, confirming that all components are essential.

The model trained with only contrastive pretraining followed by naive joint learning (c) performs worse than unimodal baselines. This observation is consistent with the earlier results on EchoMen and ConR, where multimodal joint learning leads to degraded performance. This phenomenon is consistent with our theory. Furthermore, the result of the configuration combining adaptive margin with MMPareto (d) shows that addressing only one type of imbalance is insufficient. The aggressive optimization strategy of MMPareto causes the model to jump out of the flat region of the loss landscape. Even though the adaptive margin provides a good initialization, the outcome remains similar to using MMPareto alone. Together, these findings strongly support our theory that data imbalance and learning imbalance amplify each other, and that addressing both is critical for effective multimodal regression.

**Table 2:** Ablation study on the two-stage framework. “MP” denotes the MMPareto method used in the second stage.

Method	Modal	$R^2 \uparrow$	MSE $\downarrow$	MAE $\downarrow$
Baseline	Fusion	0.371	4.64	1.52
w/o AM	Fusion	0.611	2.95	1.26
w/o SGM	OCT	0.340	4.79	1.54
	FP	0.601	2.87	1.23
	Fusion	0.525	3.21	1.29
AM w/ MP	Fusion	0.317	4.19	1.53
<b>Ours</b>	Fusion	<b>0.626</b>	<b>2.50</b>	<b>1.16</b>

**Fig. 5:** Figure A shows how gamma and sharpness change over iterations. Figure B illustrates the relationship (correlation) between the two.

## 5.5 Dynamic Sharpness-aware Modulation

Figure 5 visualizes the core mechanism of our SGM. As shown in A, the modulation factor  $\gamma$  evolves dynamically throughout training, following the measured sharpness of the local loss landscape. Here, a larger sharpness value indicates a more *peaked* (i.e., sharper) region, while a smaller value suggests a relatively *flat* region. Our key design is to couple  $\gamma$  with sharpness to enable adaptive optimization behaviors. When the sharpness increases, the loss surface becomes more rugged and sharp minima are more likely to trap the optimizer. Accordingly, SGM increases  $\gamma$  to strengthen gradient modulation, injecting stronger perturbations into the update direction and facilitating escape from sharp basins. Figure B further confirms a positive relationship between sharpness and  $\gamma$ , consistent with our design principle that modulation strength should scale with the degree of sharpness. Overall, this dynamic strategy enables SGM to react to the evolving geometry of the loss surface, enhancing robustness and stability during multimodal training.

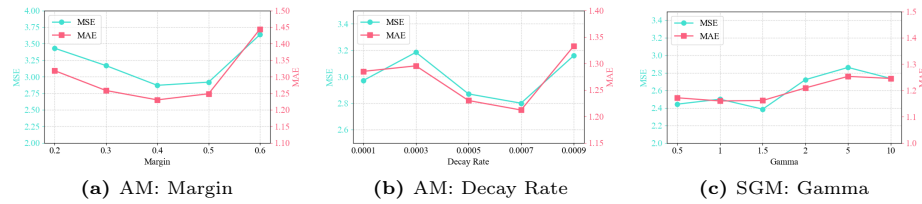


Fig. 6: Hyperparameter sensitivity analysis of AM and SGM.

## 5.6 Hyperparameter Sensitivity.

We analyze the sensitivity of key hyperparameters in AM and SGM. For AM, we vary the initial margin while fixing the decay rate to 0.0005 (Fig. 6a), and vary the decay rate while fixing the initial margin to 0.4 (Fig. 6b). For SGM, we evaluate the scaling factor  $\gamma \in \{0.5, 1, 1.5, 2, 5, 10\}$  (Fig. 6c). The results show that the performance remains stable across a wide range of hyperparameters, indicating that the proposed method is not sensitive to parameter selection.

## 6 Conclusion

In this work, we investigate the multimodal MD regression task and identify coupled imbalance issues that jointly hinder optimization. The impact of data imbalance does not lie in poor recognition of head or tail classes, but rather in the increased optimization burden it imposes on multimodal networks. This burden, coupled with the learning imbalance, makes it difficult for the network to converge effectively. We provide a theoretical explanation of why multimodal learning method fair and propose Re-M3Dr. In Re-M3Dr, this problem is decomposed into unimodal supervised contrastive learning and multimodal joint optimization. To address the ambiguous sample boundaries in long-tailed regression tasks, we propose a dynamic boundary adjustment mechanism. To improve stability under complex multimodal fusion, we design sharpness-aware gradient modulation strategy. Our approach demonstrates strong generality beyond MD regression tasks.

## References

1. Arora, K.S., Boland, M.V., Friedman, D.S., Jefferys, J.L., West, S.K., Ramulu, P.Y.: The relationship between better-eye and integrated visual field mean deviation and visual disability. *Ophthalmology* **120**(12), 2476–2484 (2013)
2. Chen, T., Kornblith, S., Norouzi, M., Hinton, G.: A simple framework for contrastive learning of visual representations. In: *International conference on machine learning*. pp. 1597–1607. PmLR (2020)
3. Foret, P., Kleiner, A., Mobahi, H., Neyshabur, B.: Sharpness-aware minimization for efficiently improving generalization. *arXiv preprint arXiv:2010.01412* (2020)

4. Keramati, M., Meng, L., Evans, R.D.: Conr: Contrastive regularizer for deep imbalanced regression. In: The Twelfth International Conference on Learning Representations
5. Keskar, N.S., Mudigere, D., Nocedal, J., Smelyanskiy, M., Tang, P.T.P.: On large-batch training for deep learning: Generalization gap and sharp minima. In: International Conference on Learning Representations (2017)
6. Koyama, M., Ueno, Y., Ito, Y., Oshika, T., Tanito, M.: Automated learning of glaucomatous visual fields from oct images using a comprehensive, segmentation-free 3d convolutional neural network model. *Scientific Reports* **15**(1), 13395 (2025)
7. Lai, S., Zhao, M., Zhao, Z., Chang, S., Yuan, X., Liu, H., Zhang, Q., Meng, G.: Echomen: Combating data imbalance in ejection fraction regression via multi-expert network. In: International Conference on Medical Image Computing and Computer-Assisted Intervention. pp. 624–633. Springer (2024)
8. Li, Z., Xing, Z., Liu, H., Zhu, L., Wan, L.: Anchored supervised contrastive learning for long-tailed medical image regression. In: Chinese Conference on Pattern Recognition and Computer Vision (PRCV). pp. 3–18. Springer (2024)
9. Lyu, X., Xu, Q., Yang, Z., Lyu, S., Huang, Q.: Sse-sam: Balancing head and tail classes gradually through stage-wise sam. In: Proceedings of the AAAI Conference on Artificial Intelligence. vol. 39, pp. 19278–19286 (2025)
10. Peng, X., Wei, Y., Deng, A., Wang, D., Hu, D.: Balanced multimodal learning via on-the-fly gradient modulation. In: Proceedings of the IEEE/CVF conference on computer vision and pattern recognition. pp. 8238–8247 (2022)
11. Phan, H., Tran, L., Tran, N.N., Ho, N., Phung, D., Le, T.: Improving multi-task learning via seeking task-based flat regions. *arXiv preprint arXiv:2211.13723* (2022)
12. Träuble, J., Hiscox, L.V., Johnson, C.L., Schönlieb, C.B., Kaminski Schierle, G.S., Aviles-Rivero, A.I.: Contrastive learning with adaptive neighborhoods for brain age prediction on 3d stiffness maps. *Transactions on Machine Learning Research* (2024)
13. Wei, Y., Hu, D.: Mmpareto: Boosting multimodal learning with innocent unimodal assistance. In: International Conference on Machine Learning. pp. 52559–52572. PMLR (2024)
14. Xu, S., Cui, M., Huang, C., Wang, H., Hu, D.: Balancebenchmark: A survey for multimodal imbalance learning. *arXiv preprint arXiv:2502.10816* (2025)
15. Yu, H.H., Maetschke, S.R., Antony, B.J., Ishikawa, H., Wollstein, G., Schuman, J.S., Garnavi, R.: Estimating global visual field indices in glaucoma by combining macula and optic disc oct scans using 3-dimensional convolutional neural networks. *Ophthalmology Glaucoma* **4**(1), 102–112 (2021)
16. Zhou, Y., Qu, Y., Xu, X., Shen, H.: Imbsam: A closer look at sharpness-aware minimization in class-imbalanced recognition. In: Proceedings of the IEEE/CVF International Conference on Computer Vision. pp. 11345–11355 (2023)
17. Zhou, Z., Li, L., Zhao, P., Heng, P.A., Gong, W.: Class-conditional sharpness-aware minimization for deep long-tailed recognition. In: Proceedings of the IEEE/CVF conference on computer vision and pattern recognition. pp. 3499–3509 (2023)
18. Zhu, Z., Wu, J., Yu, B., Wu, L., Ma, J.: The anisotropic noise in stochastic gradient descent: Its behavior of escaping from sharp minima and regularization effects. In: International Conference on Machine Learning. pp. 7654–7663. PMLR (2019)
19. Zou, K., Lin, T., Han, Z., Wang, M., Yuan, X., Chen, H., Zhang, C., Shen, X., Fu, H.: Confidence-aware multi-modality learning for eye disease screening. *Medical Image Analysis* **96**, 103214 (2024)

20. Zou, K., Lin, T., Yuan, X., Chen, H., Shen, X., Wang, M., Fu, H.: Reliable multi-modality eye disease screening via mixture of student'st distributions. In: International Conference on Medical Image Computing and Computer-Assisted Intervention. pp. 596–606. Springer (2023)